Spectrum Sensing for Powering Power Line Communications

Laryssa R. Amado, Eduarda S. C. Losqui, Fabricio P. V. de Campos,
Alvaro Augusto M. de Medeiros, and Moises V. Ribeiro

***Abstract*— The use of electric grids for communication purposes may interfere with radio communication services. To offer new directions to avoid electromagnetic interference that reduces the effectiveness of electric power grids as a green and low-cost communication channel, this paper discusses and introduces spectrum sensing techniques for cognitive power line communication (PLC) systems. Additionally, a measurement campaign for monitoring the radio spectrum in the range from 1.7 to 100 MHz is discussed as well as attained results with the spectrum sensing technique. The numerical results indicate the proposed spectrum sensing technique can offer good performance in a cognitive PLC systems.**

***Keywords*— power line communication, spectrum sensing, signal processing.**

I. INTRODUCTION

Among the available technologies, the power line communication (PLC) has emerged as an interesting candidate for what is being called smart grid communications (SGC) [1]. However, the electric power grids were not conceived for the high-frequency data communication. Also, they are not shielded and their electromagnetic radiation may interfere with radio communication services.

The potential disturbances yielded by PLC signals that could result in interference in other telecommunication systems operating in the same bandwidth, near and far from the power line cable were discussed, investigated, and measured [2]. To overcome this problem, several mitigation techniques have been proposed and introduced in some regulation and standardization documents to protect radio frequencies. The majority of these techniques are based on fixed, dynamic, and pre-fixed notching techniques [3], [4]. However, it is well known that the usability of the spectrum by primary users are time and spatial dependent and the scarcity of the spectrum for data communication, mainly for SGC, is pushing forward the introduction of cognitive concepts to improve the performance of PLC systems [3]–[6].

The use of some spectrum monitoring techniques to detect the presence of primary users was analyzed based on spectrum analyzer measurements, performed on the power line cable through a capacitive coupler or on an antenna [4], [7], [8]. Cooperative spectrum monitoring techniques are adequate to detect radio frequencies when the signal is measured directly on the power line cable [3]. Although it offers a new perspective for improving the spectrum usability for PLC systems, several questions deserve a deeper analysis for powering the PLC devices with cognitive features that result in a SGC infrastructure that guarantees QoS for smart grid, as well as electric power systems applications in the high-, medium-, and low-voltage electric grids (outdoor and indoor).

This paper aims to discuss and analyze a spectrum sensing technique for monitoring the frequency bandwidth between 1.7 and 100 MHz. In addition, this paper presents some results related to an initial measurement campaign, which was carried out in Brazil, to monitor the spectrum in the aforesaid frequency bandwidth with a setup that makes use of the spectrum sensing technique that analyzes the measured data. The results based on the measurements show that: i) the performance of the spectrum sensing technique based on the choice of transform depend upon the length of the window; ii) differently from what was pointed out [3], both signals measured with a antenna or a coupler connected to the electric grid outlet can provide detection rate higher than 99% if the suggested technique and setup are considered.

II. PROBLEM FORMULATION

Let a random and monitored signal be expressed by

$$x(t) = s(t) + v(t) = \sum_{k=1}^{K} s_k(t) + v(t), \tag{1}$$

where $s_k(t) \in \mathbb{R}$ is the signal generated by the k-th spectrum user (analog or digital); K is the number spectrum users, $v(t) \in \mathbb{R}$ is the additive noise; $x(t)$ is a time domain signal with the presence of noise. The acquisition of the signal $x(t)$ for spectrum sensing can be made by different sensors (transductor associated to an A/D device). Supposing that there are M different types of sensors, then, the use of a m-th sensor to acquire the signal $x(t)$, results in

$$\mathbf{x} = P_m(x(t)) = P_m(s(t)) + P_m(v(t)) = \mathbf{s} + \mathbf{v}, \tag{2}$$

where $\mathcal{P} = \{P_1, P_2,...,P_M\}$ defines a set of M sensors; $\mathbf{x} \in \mathbb{R}^{N\times 1}$, $\mathbf{s} \in \mathbb{R}^{N\times 1}$ and $\mathbf{v} \in \mathbb{R}^{N\times 1}$ are vectors with N coefficients, which were obtained from the signals $x(t)$, $s(t)$ and $v(t)$, respectively. Vector $\mathbf{x}$ is constituted of samples from the signal $x(t)$, which were taken at rate $f_s = 2B$, where B is the signal bandwidth, whose frequencies extend from 0 to B Hz, i.e. $f \in [0,B)$.

Laryssa R. Amado, Eduarda S. C. Losqui, Alvaro Augusto M. de Medeiros and Moises V. Ribeiro are with Department of Electrical Engineering, Federal University of Juiz de Fora Juiz de Fora, MG, 36036 900, Brazil, Email: {laryssa.amado, eduarda.losqui, alvaro, mribeiro}@engenharia.ufjf.br. Fabrício P. V. de Campos is with Electrical Engineering Program,COPPE/Federal University of Rio de Janeiro 68504, 21945-970, Rio de Janeiro, RJ, Brazil E-mail: fcampos@lps.ufrj.br.This paper was supported in part by FAPEMIG, CNPq, CAPES, CAPES-PNPD, FINEP, P&D ANEEL, and INERGE.

A linear transformation is applied to the vector $\mathbf{x}$ to explicitly show the spectral signal content of $\mathbf{s}_k$, $k = 1, 2, ..., K$, in order to sense the spectrum. Therefore, the transformed signal is expressed by

$$\mathbf{X} = \mathbf{A}_p\mathbf{x} = \mathbf{S} + \mathbf{V} = \sum_{k=1}^{K} \mathbf{S}_k + \mathbf{V} \tag{3}$$

where $\mathbf{X} \in \mathbb{C}^{N\times 1}$, $\mathbf{S}_k = \mathbf{A}_p\mathbf{s}_k \in \mathbb{C}^{N\times 1}$, $\mathbf{V}_k = \mathbf{A}_p\mathbf{v} \in \mathbb{C}^{N\times 1}$, and $\mathcal{A} = \{\mathbf{A}_1, \mathbf{A}_2, ..., \mathbf{A}_P\}$ represents a set of P spectrum transform techniques, such that $\mathbf{A}_p \in \mathbb{C}^{N\times N}$.

Note that $\mathbf{S}_k = [\mathbf{0}_{k,a}^T \; S_k(L_{a,k}) \; ... \; S_k(L_{a,k} + L_k - 1) \; \mathbf{0}_{k,b}^T]^T$, $\mathbf{0}_{k,a}$ and $\mathbf{0}_{k,b}$ are $L_{k,a}\times 1$ and $L_{k,b}\times 1$ vectors constituted by zeros, and $L_{k,a} + L_{k,b} + L_k = N$, $\forall k \in \mathbb{Z}$. By diving the vector $\mathbf{X}$ into L_q-length window, then we have

$$\mathbf{X}_{d,L_q} = \mathbf{S}_{d,L_q} + \mathbf{V}_{d,L_q} = \sum_{k=1}^{K} \mathbf{S}_{k,d,L_q} + \mathbf{V}_{d,L_q} \tag{4}$$

where $\mathbf{X}_{d,L_q} = [X((d-1)L_q) \; X((d-1)L_q + 1) \; ... \; X(L_q - 1)]^T$, is a vector constituted by L_q consecutive coefficients of the vector $\mathbf{X}$. Similarly, $\mathbf{S}_{d,L_q} = [S((d-1)L_q) \; S((d-1)L_q + 1) \; ... \; S(L_q - 1)]^T$ and $\mathbf{V}_{d,L_q} = [V((d-1)L_q) \; V((d-1)L_q + 1) \; ... \; V(L_q - 1)]^T$, where $q = 1, 2, ..., Q$. Let $\mathcal{L} = \{L_1, L_2, ..., L_Q\}$ be a set of vector lengths. Hence, the spectrum sensing problem on PLC systems can be formulated as two simple hypothesis

$$\mathbf{X}_{d,L_q} = \begin{cases} \mathbf{V}_{d,L_q}, & \mathcal{H}_0 \\ \mathbf{S}_{k,d,L_q} + \mathbf{V}_{d,L_q}, & \mathcal{H}_1 \end{cases}, \tag{5}$$

where $\mathcal{H}_0$ and $\mathcal{H}_1$ are the hypothesis associated to the absence and presence, respectively, of the k-th data communication system (narrowband or broadband). Consider a R-length feature vector, $\mathbf{r}_d \in \mathbb{R}^{R\times 1}$, extracted from $\mathbf{X}_{d,L_q}$ aiming to reduce its dimensionality. Supposing that different extraction and selection techniques are used to define the vector $\mathbf{r}_d$, then a set of features can be represented by $\mathbf{\Psi} = \Psi_1, \Psi_2, ..., \Psi_G$. Assuming that P_D (detection probability) and P_F (false alarm probability) are expressed, respectively, by $P_D = P_r(\mathbf{r}_d > \lambda|\mathcal{H}_0)$ and $P_F = P_r(\mathbf{r}_d > \lambda|\mathcal{H}_1)$, where $P_r(.)$ are the probabilities and λ is the detection threshold. The spectrum sensing problem for a PLC system can be formulated as a multi-objective problem, which can be expressed as

$$\begin{array}{c} \max P_D, \min\{P_F, \mathcal{C}, \tau\}, \\ (\mathcal{A}, \mathcal{L}, \mathcal{D}, \mathcal{P}, \Psi, \mathcal{C}, \mathcal{T}) \end{array} \tag{6}$$

where $\mathcal{A} = \{\mathbf{A}_1, \mathbf{A}_2, ..., \mathbf{A}_P\}$ is the set of transforms; $\mathcal{L} = \{L_1, L_2, ..., L_q\}$ is the set of window lengths; $\mathcal{D} = \{D_1, D_2, ..., D_U\}$ is the set of detection techniques; $\mathcal{P} = \{P_1, P_2, ..., P_M\}$ is the set of sensors; $\mathbf{\Psi} = \Psi_1, \Psi_2, ..., \Psi_G$ is the set of features; $\mathfrak{C} = \{C_1, C_2, ..., C_J\}$ is the set of computational complexities related to each choice and $\mathcal{T} = \{\tau_1, \tau_2, ..., \tau_V\}$ is the set of time intervals in which spectrum sensing should be used.

III. The Spectrum Sensing Technique

The block diagram of the detection technique used for spectrum sensing is shown in Figure 1.

Each one of the blocks can be described as:

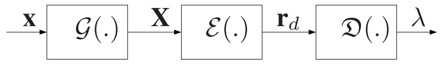

Fig. 1. Block diagram of the detection system.

- Block $\mathcal{G}(.)$: it represents the signal transformation applied to the vector $\mathbf{x}$. Due to the necessity of analyzing the frequency spectrum of this signal, the following transforms were assessed for use: DFT (Discrete Fourier Transform), DHT (Discrete Hartley Transform), DCT (Discrete Cosine Transform), DST (Discrete Sine Transform) and MCLT (Modulated Complex Lapped Transform).
- Block $\mathcal{E}(.)$: it represents the operator that first defines the vector $\mathbf{X}_{d,L_q}$ from vector $\mathbf{X}$, and then extracts the feature vector $\mathbf{r}_d \in \mathbb{R}^{R\times 1}$, such that $R \ll L_q$.
- Block $\mathfrak{D}(.)$: it implements the algorithm that provides results into states whether there is or there is not a radio signal in the vector $\mathbf{X}_{d,L_q}$.

Based on different characteristics of the signals and noise located at different parts of the selected spectrum, we suggest that the frequency bandwidth between 1.705 and 100 MHz should be divided into three sub-bands, see Figure 2-A, for spectrum monitoring application. The rationale is that those distinct frequency bands show different measured background noise levels, which can reduce the performance of the designed spectrum detection technique if only one configuration is designed to detect signal in all frequency bands.

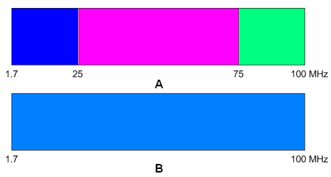

Fig. 2. The suggested spectrum division for sensing applications related to PLC system.

A. Transforms

For spectrum sensing applications, it is necessary to apply transforms to the signal, so that its spectral content becomes apparent. Therefore, any transform that provides the time $\times$ frequency representation of the signal [9] can be included in the set $\mathcal{A}$. In this context, this Section describes the following transforms: DFT, DHT, DCT, DST and MCLT, each of them were chosen because they can reveal spectrum information of the signal. It is assumed that finite length sequence is $\{x[n]\}_{n=0}^{N-1}$, such that $x[n] \in \mathbb{R}$.

The DFT is known as the standard technique for spectrum sensing. The DFT is expressed by

$$X[k] = \sum_{n=0}^{N-1} x[n]W_N^{kn}, \; 0 \le k \le N-1, \tag{7}$$

where $W_N^r = \exp\{2\pi r/N\}$.

The DHT [10] can be given by

$$X[k] = \sum_{n=0}^{N-1} x[n]cas\left(\frac{2\pi}{N}kn\right), \quad 0 \le k \le N-1, \tag{8}$$

where $cas(x) = \cos(x) + \sin(x)$.

The DCT is expressed by [10]

$$X[k] = \sum_{n=0}^{N} \alpha(n) x[n] \cos\left(\frac{(2k+1)n\pi}{2N}\right), \quad k = 0,\ 1,\ ...,\ N-1 \tag{9}$$

where

$$\alpha(n) = \begin{cases} \sqrt{\frac{1}{N}} & n = 0 \ or \ N-1 \\ \sqrt{\frac{2}{N}} & \text{otherwise} \end{cases}.$$

The DST IV is given by

$$X[k] = \sum_{n=0}^{N-1} \alpha(n) x[n] \sin\left[\frac{(2k+1)n\pi}{2N}\right], \quad k = 0,\ 1,\ ...,\ N-1 \tag{10}$$

where

$$\alpha(n) = \begin{cases} \sqrt{\frac{1}{N}} & n = 0 \text{ ou } N-1 \\ \sqrt{\frac{2}{N}} & \text{otherwise} \end{cases}.$$

The MCLT [10] is given by

$$X[k] = \sum_{n=0}^{2N-1} x[n] p[n,k],\ k = 0,\ 1,\ ...,\ N-1, \tag{11}$$

where $p[n,k]$ is a basic analysis function, defined by $p[n,k] = p_c[n,k] - jp_s[n,k]$, $j \triangleq \sqrt{-1}$, and

$$\begin{aligned} p_C[n,k] &= \sqrt{\tfrac{2}{N}} h[n] \cos\left(\left(n + \tfrac{N+1}{2}\right)\left(k + \tfrac{1}{2}\right)\tfrac{\pi}{N}\right) \\ p_S[n,k] &= \sqrt{\tfrac{2}{N}} h[n] \sin\left(\left(n + \tfrac{N+1}{2}\right)\left(k + \tfrac{1}{2}\right)\tfrac{\pi}{N}\right), \end{aligned} \tag{12}$$

in which $h[n]$ is the modulated impulse response of the filter

B. Feature Extraction Technique

Feature extraction techniques provide a large set of features related to the a vector. A premium is placed on extracting relevant features that are somewhat invariant to the change of the vector $\mathbf{x}_{d,L_q}$ in order to perform the detection. There are several kinds of feature extraction techniques for both real and complex sequences. The most common feature applied for spectrum sensing is the energy of signal due to its computational complexity and the lack of necessity of previous information about the transmitted signal [11].

In this paper, besides energy of signal, we focus on HOS- (higher order statistics), skewness-, and kurtosis-based features because they have been effective in other applications demanding detection technique [12]. Due to paper size restrictions, the expressions and details for each feature are not presented here. A summary of each of them can be found in [6].

C. Feature Selection Technique

Feature selection is a process that selects the most significant features of a set, aiming to facilitate the detection process through the use of the least possible number of features. This stage is crucial to the detection process, once it enables a better performance of this process and the design of a simpler detector.

One of the most used and simple feature extraction technique that presents reasonable results is the Fisher's Discriminant Ratio(FDR) [13]. Again, due to paper size restrictions, expressions of the FDR were suppressed. A more detailed presentation of the use of FDR on spectrum sensing purposes can be found in [6].

D. Detection Technique

After reducing the dimensionality of the vector $\mathbf{x}_{d,L_q}$, we ought to test whether the chosen detector is suitable to this problem or not. There are several detection techniques based on detection theory. However, the analysis of the histogram of the extracted feature vector reveals how complicated it can be to fit into a distribution model. In fact, although the number of measurement are representative, we believe that much more measurements need to be carried out to provide a representative set of monitored signals, from which the distribution of feature vector can be obtained. Therefore, in this paper, we have chosen the Multi-Layer Perceptron Neural Network (MLPNN) and a training procedure highlighted in [14], because it had provided good performance in detection and classification problems related to other applications. Due to limitation on number of pages, the expressions for the MPLNN are not presented here, but they can be found in [6].

IV. The Spectrum Measurement Campaign

The measured data were acquired by the acquisition board Gage Razor CompuScope 1642 [15], which consists of several analog-to-digital converters of 16 bits of vertical resolution with maximum sampling rate of 200 MS/s by channel.

Two kind of sensors were used to acquire the spectrum signal: i) an omnidirectional antenna with bandwidth raging from 1 MHz up to 1000 MHz and impedance equals 50 Ω, and ii) a capacitive coupler (PREMO P-1240-021) [16], which introduces an increasing attenuation when the frequency goes beyond 30 MHz and owns a high-pass filter with cutoff frequency f_c =1.7 MHz.

Two input channels of the acquisition board were used to measure the signal with the antenna and capacitive coupler simultaneously. The simultaneous acquisition of the spectrum signal with the aforementioned sensors (transducers) aims to provide an answer to the investigation question #1.

The measurements were made at 16 different locations in the city of Juiz de Fora, during the morning, afternoon and evening, to capture different influences, since it is known that the spectrum influences vary with time and space as well. In each period of time, 100 measurements were taken every 6 seconds, an empirically determined interval. On total, 4800 measurements were taken and each measure is constituted by 8192 samples. The places are close to airport, army facilities and urban areas (home and building of low- and medium-income habitants).

The time-dependence of the spectrum can be observed in Figures 3, 4 and 5. Note that during the morning a very specific kind of source of disturbance yielded a noise that corrupted the spectrum. Also, only during the evening hours the army made use of the frequency bandwidth around 40 MHz for data communications, what reveals that the use of spectrum sensing technique can maximize the usability of these frequency bandwidth. Additionally, it could be verified that several bands allocated to some radio communication systems are scarcely used.

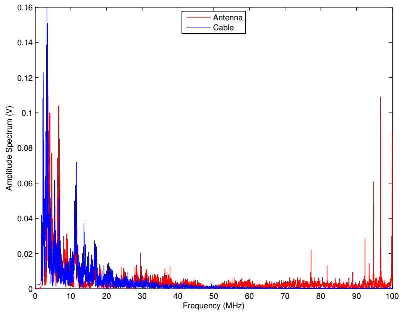

Fig. 3. The amplitude spectrum, based on DFT, of a signal measured with the antenna in the downtown in the morning.

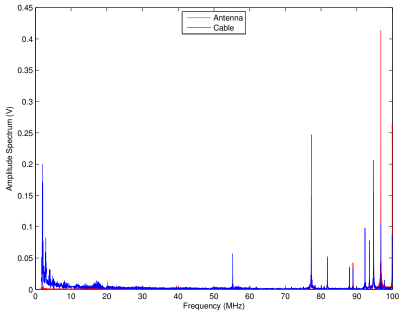

Fig. 4. The amplitude spectrum, based on DFT, of a signal measured with the antenna in downtown in the afternoon.

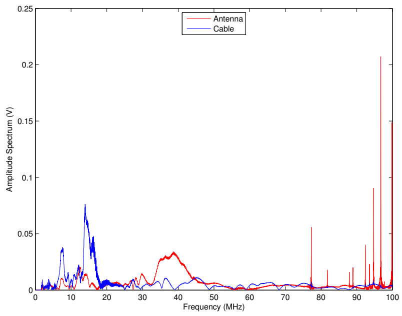

Fig. 5. The amplitude spectrum, based on DFT, of a signal measured with the antenna in downtown in the evening.

V. Numerical Results

A. Measured Data

The following considerations were taken into account for measuring the spectrum signals as well as to design the spectrum sensing technique: B =100 MHz, N =8192, and R =3. Tables I, III, and V show the results obtained for the measurements made on the antenna, while Tables II, IV, and VI display the results for the measurements made on the cable, using the capacitive coupler.

The detection rates for signals from 1.705 MHz up to 25 MHz measured on the antenna and coupler are shown in Table I and II. It can be seen that on the average the DST and DCT provide the best performance in terms of detection rate while the DFT the worst one. Overall, the best performances were attained when L_q =128 and L_q =256.

The interval from 25 MHz to 75 MHz, for the data measured on the antenna and coupler, the highest detection rate, 99.27%, happens for the DST, when L_q =32, as shown in Table III. The window size that most frequently led to the best result for each transform was L_q =32. In Table IV, the highest detection rate is related to the DCT and $L_q = 16$. However, the window sizes that show the best results for each transform are L_q =128 and L_q =256.

TABELA I

Detection rates for the measurements made using the antenna (%) - Sub-band #1.

Transforms	$L_q = 16$	$L_q = 32$	$L_q = 128$	$L_q = 256$
DFT	95.27	96.54	98.55	97.27
MCLT	98.72	98.36	95.81	98.18
DHT	90.91	98.72	98.91	98.91
DCT	98.91	98.91	98.91	98.91
DST	97.09	90.45	99.63	99.45

TABELA II

Detection rates for the measurements made on the cable (%) - Sub-band #1.

Transforms	$L_q = 16$	$L_q = 32$	$L_q = 128$	$L_q = 256$
DFT	89.45	96.91	89.45	92.00
MCLT	95.63	89.27	96.36	77.45
DHT	96.18	94.18	97.09	88.72
DCT	97.63	99.27	78.91	99.45
DST	98.91	98.18	91.09	99.82

TABELA III

Detection rates for the measurements made on the antenna (%) - Sub-band #2.

Transforms	$L_q = 16$	$L_q = 32$	$L_q = 128$	$L_q = 256$
DFT	98.00	97.45	95.09	97.45
MCLT	86.72	98.36	97.09	98.36
DHT	97.09	95.81	96.72	98.00
DCT	99.09	98.55	99.09	98.36
DST	98.54	99.27	96.18	95.54

TABELA IV

Detection rates for the measurements made on the cable (%) - Sub-band #2.

Transforms	$L_q = 16$	$L_q = 32$	$L_q = 128$	$L_q = 256$
DFT	98.00	96.18	95.27	94.72
MCLT	95.81	97.63	93.81	97.27
DHT	90.36	98.00	98.72	96.00
DCT	97.81	98.72	98.54	99.27
DST	99.27	98.91	85.82	98.00

The last part of the spectrum detection rate for the antenna measured data is shown in Table V, and the highest rate P_D =100% was calculated for the DCT transform, when L_q =256. The last part of the spectrum of the measurements made on the cable has its results exposed in Table VI. In this case, the DCT has $P_D = 100$% for L_q =16 and 32. These are indeed, the window sizes that presented the best results for all transforms.

In general, it can be stated that for the first part of the spectrum, for both the measurements made on the antenna and on the cable, the window size L_q =128 shows the best

TABELA V

DETECTION RATES FOR THE MEASUREMENTS MADE ON THE ANTENNA (%) - SUB-BAND #3.

Transforms	$L_q = 16$	$L_q = 32$	$L_q = 128$	$L_q = 256$
DFT	95.63	98.91	98.00	94.36
MCLT	98.54	99.09	97.72	89.09
DHT	94.73	98.19	98.00	96.36
DCT	99.27	87.09	99.09	100.00
DST	98.09	91.81	98.00	99.63

TABELA VI

DETECTION RATES FOR THE MEASUREMENTS MADE ON THE CABLE (%) - SUB-BAND #3.

Transforms	$L_q = 16$	$L_q = 32$	$L_q = 128$	$L_q = 256$
DFT	97.09	98.54	97.81	96.91
MCLT	96.72	96.18	98.36	94.36
DHT	97.82	98.54	96.36	94.54
DCT	100.00	100.00	96.00	99.45
DST	99.45	99.81	50.00	74.18

results on most of the measured data, which is plausible if it is analyzed that this part has signals with proportionally wider bandwidths, and consequently need detection windows with higher bandwidth. In the second sub-band, the L_q that presented best results can not be identified, due to the variability of bandwidths found in different measurements. In the third sub-band, the window sizes that present best results are L_q =16 and 32. The reason for this lies in the fact that the measured signals on this sub-band by both sensors are narrowband, and large windows cannot capture them properly.

Tables VII and VIII present the detection rates for measurements for the whole spectrum (see Figure 2-B) using antenna and cable, respectively. On the former results, it can be noticed that the higher detection rates occur when data are obtained from the DHT and DST transforms and window sizes 256 and 128, while on the latter results, the higher detection rate occurs when the DST and DCT transforms and L_q =16. On both Tables, we can also observe that the DFT presents the worst detection rates on both scenarios. Also, Tables VII and VIII reveal that the attained results are lower than those obtained with the frequency division suggested in Figure 2-A (see Tables I-VI).

TABELA VII

DETECTION RATES FOR THE MEASUREMENTS MADE ON THE ANTENNA (%) - WHOLE SPECTRUM.

Transforms	$L_q = 16$	$L_q = 32$	$L_q = 128$	$L_q = 256$
DFT	93.16	96.83	89.33	82.67
MCLT	97.83	99.00	93.00	93.00
DHT	97.33	95.67	97.33	99.33
DCT	98.5	97.83	97.5	98.5
DST	98.5	98.17	99.17	97.17

The best detection rates were obtained for the measurements made on both cable and antenna. Then, we can not state, based on our work, which sensor can provide the best performance.

VI. CONCLUDING REMARKS

This paper discussed and investigated some relevant aspects related to spectrum sensing technique for powering PLC systems. Also, it introduced a spectrum sensing technique and, based on several assumptions and constraints, analyzed its performance based on measured data. Overall, the attained results indicate that the proposed technique is effective for spectrum sensing and gives some directions for the design of cognitive PLC systems. Finally, it can be concluded that the use of the spectrum by PLC systems can be enhanced by applying spectrum sensing techniques, such as the one discussed in this contribution.

TABELA VIII

DETECTION RATES FOR THE MEASUREMENTS MADE ON THE CABLE (%) - WHOLE SPECTRUM.

Transforms	$L_q = 16$	$L_q = 32$	$L_q = 128$	$L_q = 256$
DFT	91.67	97.5	86.00	62.3
MCLT	93.00	97.5	86.33	82.5
DHT	96.67	91.67	96.83	66.83
DCT	98	97.33	97.33	96.83
DST	98.67	94.17	97.5	98.33

REFERÊNCIAS

[1] S. Galli, A. Scaglione, and Z. Wang, "For the grid and through the grid: The role of power line communications in the smart grid," *Proceedings of the IEEE*, vol. 99, no. 6, pp. 998–1027, June 2011.

[2] Y. R. Ferreira, "Inspection method on measuring unwanted emissions from broadband power line using mobile monitoring station," in *IEEE International Symposium on Power Line Communications and Its Applications*, Mar. 2010, pp. 231–235.

[3] B. Praho, M. Tlich, P. Pagani, A. Zeddam, and F. Nouvel, "Cognitive detection method of radio frequencies on power line networks," in *IEEE International Symposium on Power Line Communications and Its Applications*, 2010.

[4] P. Pagani, R. Razafferson, A. Zeddam, B. Praho, M. Tlich, J. Baudais, A. Maiga, O. Isson, G. Mijic, K. Kriznar, and S. Drakul, "Electro magnetic compatibility for power line communications," in *IEEE 21st International Symposium on Personal Indoor and Mobile Radio Communications*, 2010, pp. 2799–2804.

[5] S. W. Oh, Y. L. Chiu, K. N. Ng, R. Mo, Y. Ma, Y. Zeng, and A. A. S. Naveen, "Cognitive power line communication system for multiple channel access," in *IEEE International Symposium on Power Line Communications and Its Applications*, Apr. 2009, pp. 47–52.

[6] L. R. Amado, "Uma contribuição à análise de técnicas de monitoramento de espectro para sistemas plc," M.S. thesis, Universidade Federal de Juiz de Fora, Aug. 2011.

[7] I. S. Areni, S. Tsuzuki, and Y. Yamada, "A study of radiation detection methods for cognitive plc system," in *IEEE International Symposium on Power Line Communications and Its Applications*, 2011, pp. 430–433.

[8] N. Weling, "Feasibility study on detecting short wave radio stations on the powerlines for dynamic psd reduction as method for cognitive plc," in *IEEE International Symposium on Power Line Communications and Its Applications*, Apr. 2011, pp. 311–316.

[9] S. Haykin, D. J. Thomson, and J. H. Reed, "Spectrum sensing for cognitive radio," in *Proceedings of the IEEE*, May 2009, vol. 97, pp. 849–877.

[10] H. S. Malvar, *Signal processing with lapped transforms*, Artech House, 1957.

[11] M. C. V. I. F. Akyildiz, W. Y. Lee, and S. Mohanty, "NeXt generation/dynamic spectrum access/cognitive radio wireless networks: A survey," *Computer Networks*, vol. 50, no. 13, pp. 2127–2159, Sep. 2006.

[12] M. V. Ribeiro, C. A. G. Marques, C. A. Duque, A. S. Cerqueira, and J. L. R. Pereira, "Detection of Disturbances in Voltage Signals for Power Quality Analysis Using HOS," *EURASIP Journal on Advances in Signal Processing*, vol. 2007, 2007, ID 59786, 13 pages.

[13] S. Theodoridis and K. Koutroumbas, *Pattern Recognition*, Elsevier, 2nd edition, 2003.

[14] S. Haykin, *Neural Networks - Comprehensive Foundation*, Pearson Education, 2nd edition, 1999.

[15] Gage, "Razor compuscope 16XX," www.gage-applied.com, 2011.

[16] PREMO, "Capacitive Coupler P-1240-021," www.grupopremo.com, 2011.